Probing the Intergalactic Magnetic Field with the Anisotropy of the Extragalactic Gamma-ray Background

T. M. Venters[1]* and V. Pavlidou[2,3]

[1] *Astrophysics Science Division, NASA Goddard Space Flight Center, Greenbelt, MD, 20771, USA*
[2] *Max-Planck Institute for Radio Astronomy, Auf dem Hügel 69, DE-53121, Bonn, Germany*
[3] *Department of Physics, University of Crete, 71003 Heraklion, Greece*

19 January 2012

ABSTRACT

The intergalactic magnetic field (IGMF) may leave an imprint on the anisotropy properties of the extragalactic gamma-ray background, through its effect on electromagnetic cascades triggered by interactions between very high energy photons and the extragalactic background light. A strong IGMF will deflect secondary particles produced in these cascades and will thus tend to isotropize lower energy cascade photons, thus inducing a modulation in the anisotropy energy spectrum of the gamma-ray background. Here we present a simple, proof-of-concept calculation of the magnitude of this effect and demonstrate that the two extreme cases (zero IGMF and IGMF strong enough to completely isotropize cascade photons) would be separable by ten years of *Fermi* observations and reasonable model parameters for the gamma-ray background. The anisotropy energy spectrum of the *Fermi* gamma-ray background could thus be used as a probe of the IGMF strength.

Key words: magnetic fields – gamma rays: diffuse background – gamma rays: galaxies – galaxies: star formation – galaxies: active – BL Lacertae objects: general

1 INTRODUCTION

Cosmic magnetic fields are expected to play a fundamental role in the physics of a large variety of astrophysical systems. The fate of high energy particles, such as ultra-high energy cosmic rays, as they propagate through the Universe and the acceleration of charged particles in astrophysical objects hinge, in large part, on magnetic fields within their sources and those permeating the Universe. Large-scale magnetic fields such as those found in galaxies and clusters of galaxies have been a mystery for the past several decades. While they are generally thought to be the result of the amplification of weak seed fields, the origins of these seed fields, whether they be cosmological or astrophysical in nature, are largely unknown. A definitive measurement of the intergalactic magnetic field (IGMF) could provide a fundamental step in resolving the questions of the origins of cosmic magnetic fields and their impact on the evolution of the systems in which they reside, but sufficiently constraining observations have thus far remained elusive. Previously, upper bounds of $\sim 10^{-9}$ G have been found through Faraday rotation limits of polarized radio emission from distant quasars and the study of the effect of magnetic fields on the anisotropy of the cosmic microwave background (for a brief review of observational and theoretical techniques to constrain the IGMF, see e.g., Neronov & Semikoz 2009, and references therein). The recent availability of data from the *Fermi* Large Area Telescope (LAT) has renewed interest in the IGMF as observations of the gamma-ray sky and its participating source populations provide a unique perspective on the strength and structure of the IGMF.

The gamma-ray sky consists of resolved point sources (such as normal galaxies and active galaxies, pulsars, etc.), transient gamma-ray sources (e.g., gamma-ray bursts), and the diffuse gamma-ray radiation comprised of emission from the Galaxy and the isotropic (presumably, extragalactic) gamma-ray background (EGB). The EGB is a window into the high-energy processes in the Universe the origins of which have been the subject of much debate; however, it is expected that emission arising from unresolved, extragalactic point sources, such as blazars and star-forming galaxies, comprises a sizable contribution to the EGB (see e.g., Stecker & Salamon 1996; Fields et al. 2010; Abdo et al. 2010d; Stecker & Venters 2011, and references therein). Additionally, many of these extragalactic point sources are also sources of very-high energy (VHE) gamma rays,[1] which in-

---

*E-mail: tonia.m.venters@nasa.gov; pavlidou@mpifr-bonn.mpg.de

[1] In this paper, we take VHE to be $\sim$ TeV.

teract with the soft photons of the extragalactic background light (EBL), consisting of the cosmic microwave background (CMB) and the background of infrared, optical, and ultraviolet radiation from direct and dust-reprocessed starlight. The interactions of VHE photons with the EBL initiate electromagnetic (EM) cascades, giving rise to another contribution to the EGB (see e.g., Coppi & Aharonian 1997; Kneiske & Mannheim 2008; Inoue & Totani 2009; Venters 2010). However, the degree to which astrophysical sources contribute to the EGB depends on their distribution with respect to luminosity and redshift (the gamma-ray luminosity function, GLF), their intrinsic spectra at gamma-ray energies, and the nature of the EBL, all of which remain the subjects of intense debate (see e.g., Venters 2010; Fields et al. 2010; Abdo et al. 2010b,d; Makiya et al. 2011; Inoue 2011; Stecker & Venters 2011; Abazajian et al. 2011).

A promising complimentary technique for investigating the contributions of astrophysical sources to the EGB involves studying its intensity anisotropy properties as a function of energy. As pointed out in Siegal-Gaskins & Pavlidou (2009; see also Hensley et al. 2010; Siegal-Gaskins et al. 2011), the contribution of a given class of sources to the overall fluctuation angular power at a given angular scale of the EGB at a given energy is weighted by the square of its fractional contribution to the intensity of the EGB at that energy. As such, if the relative contributions of the various EGB contributors change with energy, so too will the angular power as a function of energy. Expectations for the anisotropies of the commonly invoked astrophysical contributors to the EGB are that star-forming galaxies contribute very little anisotropy owing to the fact that they are so numerous and individually faint, while blazars, being far more rare than star-forming galaxies but much brighter, could have a large contribution to the EGB anisotropy (Ando et al. 2007; Ando & Pavlidou 2009; Siegal-Gaskins & Pavlidou 2009; Hensley et al. 2010; Cuoco et al. 2011). It has also been suggested that annihilation in dark matter substructure in the Galactic halo could also have a large contribution to the EGB anisotropy, even if the contribution to the EGB intensity from dark matter annihilation is subdominant with respect to other contributions (see e.g., Ando et al. 2007; Siegal-Gaskins 2008; Taoso et al. 2009; Ando 2009; Siegal-Gaskins & Pavlidou 2009; Hensley et al. 2010). Early anisotropy results from the _Fermi_-LAT Collaboration (Cuoco et al. 2011) suggest that the energy dependence of the intensity anisotropy of the EGB may be consistent with arising from a source population with spectra similar to that of blazars ($\alpha \sim 2.4$), even though blazars may comprise $\lesssim 30\%$ of the EGB intensity (Abdo et al. 2010d). Thus, even contributions to the EGB that are subdominant with respect to other contributions can have a profound impact on the anisotropy of the EGB, especially if its fractional contribution changes with energy. As such, it could prove a powerful tool in detecting changes in the EGB anisotropy resulting from the magnetic deflection of EM cascades from blazars.

In interacting with EBL photons, VHE gamma rays initiate EM cascades of photons, electrons, and positrons. The interaction of a VHE gamma ray with an EBL photon produces a pair of electrons and positrons, which will, in turn, Inverse Compton scatter EBL photons to high energies. These up-scattered photons will, in turn, pair produce,

and the process continues until the energies of the resulting photons are low enough that pair production is no longer efficient. In the presence of an IGMF, the charged particles in the cascade are deflected away from the direction of propagation of the primary photon. As these charged particles propagate through the EBL, they can up-scatter soft photons into the line of sight of the observer, though they will appear to be coming from a different direction. Observationally, this process results in a "halo" of gamma rays around the source. The detection of a halo around a gamma-ray point source would not only provide strong evidence for an IGMF, but would also provide an indication of the strength of the IGMF. Several groups have already conducted searches for extended emission around gamma-ray sources (see e.g., Aharonian et al. 2001; Neronov & Vovk 2010; Ando & Kusenko 2010; Aleksić et al. 2010; Neronov et al. 2011), though as yet, no significant indication of gamma-ray halos distinguishable from instrumental effects have been reported. However, the absence of significant halo emission could imply a strong IGMF that would extend the EM cascade halo such that the surface brightness of the extended source falls below the detection threshold (Neronov & Vovk 2010; Ando & Kusenko 2010). In addition to possibly creating a halo, the deflection of EM cascades by the IGMF could result in a reduction in observable cascade radiation. Analyses employing simultaneous observations of blazars by Atmospheric Cherenkov Telescopes and _Fermi_ make use of this fact to derive limits on the IGMF (Dermer et al. 2011; Essey et al. 2011; Taylor et al. 2011). These techniques are quite promising and, with more data from _Fermi_, will continue to shed light on the IGMF. In this paper, we consider a different promising technique that makes use of the anisotropy energy spectrum of the EGB to constrain the IGMF.

For any cosmological population, such as blazars, that emits gamma rays at very high energies, the effect of EM cascading results in a flux suppression at the highest energies and enhancement at lower energies as the cascades redistribute radiation from the higher energies to the lower energies (Coppi & Aharonian 1997; Kneiske & Mannheim 2008; Inoue & Totani 2009; Venters 2010). In considering the spectral subpopulations of blazars, flat-spectrum radio quasars (FSRQs) and BL-Lacertae type objects (BL Lacs), the intrinsic spectra of FSRQs is much softer than that of both BL Lacs and EM cascades, and their relative prominence with respect to the EGB can change with energy (Venters 2010; Venters & Pavlidou 2011). As such, the fluctuation angular power in the EGB should change with energy _even if FSRQs and BL Lacs have similar anisotropy properties_. Furthermore, as noted earlier, the deflection of EM cascades by the IGMF can spatially extend the emission around gamma-ray sources and reduce the observable cascade radiation. Thus, the impact of a strong IGMF is to _reduce_ the blazar anisotropy both because of the increased angular scale of the sources and because of the reduction in the overall blazar contribution to the EGB (assuming that blazars are the most anisotropic EGB component). On the other hand, in the absence of a strong IGMF, the EM cascades are highly collimated in the direction of the primary photon ($\delta \sim m_e/E_e$; Neronov & Semikoz 2009), and their impact on the blazar anisotropy is to _reinforce_ it due to the enhancement in the overall blazar contribution to the EGB. Hence, in the two extreme cases for the IGMF, EM cascades

could have a profound and *opposite* impact on the blazar anisotropy and, by extension, the EGB anisotropy. Therefore, studies of the EGB anisotropy could prove a sensitive probe into the nature of the IGMF.

In this paper, we explore the impact of EM cascade radiation from blazars on the IGRB anisotropy in the extreme cases of a negligible IGMF and a strong enough IGMF to essentially isotropize the cascade emission (i.e., from the *observationally* practical standpoint). This study is meant to serve as a proof of concept for the feasibility of using IGRB anisotropies as an IGMF probe. In Section 2, we present the methodology and parameters employed to determine the anisotropy energy spectrum and the EM cascades. In Section 3, we present the results of the calculation. In Section 4, we discuss our results and conclude.

2 METHODOLOGY & INPUTS

2.1 Collective Intensity of Unresolved Astrophysical Sources

The contribution to the EGB due to unresolved blazars can be viewed as the superposition of the collective intensity of *intrinsic* blazar spectra and the contribution from the cascade radiation from the interactions of VHE photons from blazars with the EBL:

$$I_E^{\text{bl}}(E_0) = I_E^i(E_0) + I_E^c(E_0) , \tag{1}$$

where the intensity, $I_E(E_0)$, is given in units of photons per unit area per unit time per unit solid angle per unit energy emitted at observer frame energy, E_0. In calculating the collective spectrum of unresolved blazars, we follow the formalism as outlined in Venters & Pavlidou (2011). Blazar spectra are taken to be smoothly broken power laws:

$$F_E(E_0) = F_0 \left[\left(\frac{E_0}{E_b} \right)^{\alpha_1 n} + \left(\frac{E_0}{E_b} \right)^{\alpha_2 n} \right]^{-1/n} , \tag{2}$$

where $F_E(E_0)$ is the differential photon flux in units of photons per unit area per unit energy per unit time, E_b is the break energy, $\alpha_1 = \alpha - \Delta\alpha_1$ is the low-energy slope, $\alpha_2 = \alpha + \Delta\alpha_2$ is the high-energy slope, α is the gamma-ray photon spectral index of the blazar assuming an unbroken power-law spectrum,[2] and n quantifies the sharpness of the transition from the low-energy power law to the high-energy power law (taken to be 1).

The total flux, F, of photons with energies greater than some fiducial energy, E_f (taken to be 100 MeV), is found by integrating $F_E(E_0)$ over energy,

$$F = F_0 \int_{E_f}^{\infty} \left[\left(\frac{E_0}{E_b} \right)^{\alpha_1} + \left(\frac{E_0}{E_b} \right)^{\alpha_2} \right]^{-1} dE_0 . \tag{3}$$

Then, the contribution of a single unresolved blazar to the EGB is

$$I_1 = \frac{F \left[(E_0/E_b)^{\alpha_1} + (E_0/E_b)^{\alpha_2} \right]^{-1}}{4\pi \int_{E_f}^{\infty} \left[(E_0/E_b)^{\alpha_1} + (E_0/E_b)^{\alpha_2} \right]^{-1} dE_0} \tag{4}$$

where the flux of one source is uniformly distributed over

the entire sky in anticipation of an isotropically distributed cosmological population. Including absorption due to the EBL, the contribution becomes

$$I_1 = \frac{F \left[(E_0/E_b)^{\alpha_1} + (E_0/E_b)^{\alpha_2} \right]^{-1}}{4\pi \int_{E_f}^{\infty} \left[(E_0/E_b)^{\alpha_1} + (E_0/E_b)^{\alpha_2} \right]^{-1} dE_0} e^{-\tau(E_0,z)} \tag{5}$$

where $\tau(E_0, z)$ is the optical depth for a photon with observer frame energy, E_0, emitted at redshift, z. In determining the total unresolved blazar contribution including EBL absorption, one would generally rewrite Equation 5 in terms of the blazar gamma-ray luminosity and redshift, multiply by the blazar GLF and *intrinsic* spectral index distribution (corrected for the spectral bias endemic to flux-limited surveys[3] as per Venters et al. (2009)), and finally integrate over gamma-ray luminosity, redshift, and spectral index (see e.g., Venters et al. 2009). However, since the focus of this paper is to study the relative changes with energy in the EGB anisotropy, we do not fully calculate the unresolved blazar contribution to the EGB. Rather, we assume typical luminosities and redshifts for all blazars. As such, the only integral that must be performed is that over the spectral index:

$$I_E^{\text{bl}}(E_0) =$$
$$I_0 \int_{-\infty}^{\infty} d\alpha\, p(\alpha) \frac{[(E_0/E_b)^{\alpha_1} + (E_0/E_b)^{\alpha_2}]^{-1}}{\mathcal{S}(E_f, \alpha)} e^{-\tau(E_0,z)} , \tag{6}$$

where I_0 is a normalization constant, $p(\alpha)$ is the *measured* spectral index distribution (SID), and

$$\mathcal{S}(E_f, \alpha) = \int_{E_f}^{\infty} dE_0 \left[\left(\frac{E_0}{E_b} \right)^{\alpha_1} + \left(\frac{E_0}{E_b} \right)^{\alpha_2} \right]^{-1} . \tag{7}$$

We fix the normalization constant such that the total astrophysical (blazars, star-forming galaxies, and EM cascades) contribution to the EGB fits the spectrum of the EGB as measured by the *Fermi*-LAT (Abdo et al. 2010c). In determining the measured SID, we make use of the results presented in Venters & Pavlidou (2011) from a likelihood analysis fitting *Fermi*-LAT First Catalog (Abdo et al. 2010e) FSRQs and BL Lacs to Gaussian SIDs accounting for errors in measurement of individual blazar spectral indices. For these blazar subpopulations, the maximum-likelihood Gaussian SIDs can be characterized by means (α_0) and spreads (σ_0) with parameters determined to be $\alpha_0 = 2.45$ and $\sigma_0 = 0.16$ for FSRQs and $\alpha_0 = 2.17$ and $\sigma_0 = 0.23$ for BL Lacs. Following Venters & Pavlidou (2011), we model the spectral breaks by taking $\Delta\alpha_1 = 0.1$, $\Delta\alpha_2 = 0.9$, and $E_{b,0} = 4$ GeV for FSRQs. For BL Lacs, we take $E_{b,0} = 10$ TeV. Since the AGN population peaks ~ 1, we take the typical redshift of blazars to be $z_{\text{src}} = 1$. In modeling the suppression of the source brightness due to magnetic deflection of cascades (see Appendix), we take the jet opening angle of blazars to be $\sim 1°$. The model of the EBL was taken from Franceschini et al. (2008).

We also include a model of the star-forming galaxy (SF) contribution to the EGB. In this case, we assume that the

---

[2] For the sake of clarity, we use α for the photon index rather than Γ, which is commonly used in the literature.

[3] We note that the *Fermi* survey is not exactly a flux-limited survey due to the non-uniformity of the total diffuse background throughout the sky. However, for the purposes of this paper, we neglect this effect.

gamma-ray luminosity of an SF galaxy is mainly due to the decay of neutral pions created through galactic cosmic-ray interactions with neutral hydrogen in the galaxy. It is thought that galactic cosmic rays are accelerated in supernova remnants and then diffuse throughout the galaxy. Hence, the flux of galactic cosmic rays is expected to be proportional to the galaxy's supernova rate, which is, in turn, proportional to its star-formation rate. Furthermore, the neutral hydrogen gas provides the fuel for forming stars. As such, the expectation is that an SF galaxy's gamma-ray luminosity can be parameterized in terms of its star-formation rate (Pavlidou & Fields 2002; Abdo et al. 2010a; Fields et al. 2010; Makiya et al. 2011; Stecker & Venters 2011). For the purposes of this paper, we model the star-forming galaxy contribution using the infrared luminosity function model of Stecker & Venters (2011). In this model, the star-formation rate of an SF galaxy is assumed to be proportional to its infrared luminosity; thus, the gamma-ray luminosity of an SF galaxy is proportional to a power

of its infrared luminosity. In Stecker & Venters (2011), the relationship between the gamma-ray luminosity of an SF galaxy and its infrared luminosity was determined by fitting the measured gamma-ray luminosities of *Fermi*-detected SF galaxies to their infrared luminosities. The SF galaxy contribution could then be determined by integrating over an infrared luminosity function of SF galaxies, which they took from Hopkins et al. (2010).

2.2 Electromagnetic Cascades from Blazars

The cascade intensity is given by

$$I_E^c = \frac{d^4 N^c}{dt dA d\Omega dE} \, , \qquad (8)$$

where dN^c/dE is the spectrum of cascade photons due to pair production and Inverse Compton scattering (for full equations and derivations, see Venters 2010):

$$\frac{dN^c}{dE_0}(E_0) = \int_0^{z_{\max}} \int_{E_{p,\min}}^{E_{p,\max}} (1+z) \frac{d^2 N_\gamma}{dz dE_p} P(f; E_p, z) \left[\frac{dN_{\Gamma_1}(E_0(1+z))}{dE} + \frac{dN_{\Gamma_2}(E_0(1+z))}{dE} \right] e^{-\tau(E_0, z)} dE_p dz \, , \qquad (9)$$

where dN_Γ/dE is the spectrum of Inverse Compton scattered radiation per electron of Lorentz factor, Γ, $P(f; E_p, z)$ is the probability that the pair production interaction at a given redshift, z, of a primary photon of energy E_p will produce electron-type particles of energies $E_{e1} = f \times E_p$ and $E_{e2} = (1-f) \times E_p$, $\Gamma_1 = f \times E_p/mc^2$, $\Gamma_2 = (1-f) \times E_p/mc^2$, and $d^2 N_\gamma/dz dE_p$ is the continuous spectrum of photons undergoing pair production interactions as a function of redshift and primary energy.

The full numerical integration of Equation 9 is computationally cumbersome. As such, in order to calculate the

cascade spectrum, one typically makes use of a Monte Carlo code, such as *Cascata* (Venters 2010), that propagates photons from known spectra and redshift distributions and calculates the cascade spectrum of each photon. However, for the purposes of this paper, we employ a more semi-analytical model of the cascade development. Since we have assumed a typical redshift for all blazars, we have eliminated the need for randomly generated source redshifts. Instead, the spectrum of pair-producing photons, $d^2 N_\gamma/dz dE_p$, can readily be determined from the *absorbed* collective intensity of unresolved blazars binned in energy:

$$\int_{E_{0,\min}}^{E_{0,\max}} I_E^{\mathrm{abs}}(E_0) dE_0 = I_0 \int_{E_{0,\min}}^{E_{0,\max}} \int_{-\infty}^{\infty} d\alpha \, p(\alpha) \frac{[(E_0/E_b)^{\alpha_1} + (E_0/E_b)^{\alpha_2}]^{-1}}{\mathcal{S}(E_f, \alpha)} \left(1 - e^{-\tau(E_0, z)} \right) dE_0 \, . \qquad (10)$$

For each energy bin, we determined a characteristic redshift for the start of the cascades based on the criterion that the characteristic redshift is that at which the number of photons that have been "absorbed" in propagating from the source redshift is half the number of the total photons "absorbed" in propagating to the present epoch. Using this criterion, the characteristic redshift can be calculated numerically from

$$\tau_*(E_0, z_*) = \ln \left[\frac{1}{2} \left(e^{\tau(E_0, z_{\mathrm{src}})} + 1 \right) \right] \, . \qquad (11)$$

Also, we assume that each secondary electron produced in a pair-production interaction carries half of the energy of the primary photon. Finally, since the number density of CMB photons is much higher than those of the other wavelengths that comprise the EBL, we assume that the seed photons for

the Inverse Compton interactions are CMB photons. In so doing, we can neglect Klein-Nishina effects in determining the spectrum of scattered radiation. The spectrum of scattered radiation per electron of Lorentz factor, Γ is given by (Venters 2010)

$$\frac{dN_\Gamma}{d\epsilon_1} = \int \frac{d^3 N_{\Gamma'}}{dt d\epsilon_1 d\epsilon} dt d\epsilon = \int \frac{d^3 N_{\Gamma'}}{dt d\epsilon_1 d\epsilon} \left| \frac{dt}{dE_e} \right| dE_e d\epsilon \, , \qquad (12)$$

where Γ' is the electron Lorentz factor at time, t, ϵ is the initial soft photon energy, ϵ_1 is the scattered photon energy, $d^3 N_{\Gamma'}/dt d\epsilon_1 d\epsilon$ is the differential scattered photon spectrum given by (Blumenthal & Gould 1970)

$$\frac{d^3 N_{\Gamma'}}{dt d\epsilon_1 d\epsilon} = \frac{3 \sigma_T c}{16 \Gamma'^4} \frac{n(\epsilon)}{\epsilon^2} \left(2\epsilon_1 \ln \frac{\epsilon_1}{4 \Gamma'^2 \epsilon} + \epsilon_1 + 4 \Gamma'^2 \epsilon - \frac{\epsilon_1^2}{2 \Gamma'^2 \epsilon} \right) \, , \qquad (13)$$

$n(\epsilon)d\epsilon$ is the number density of soft photons, and $|dE_e/dt|$ is the rate of energy loss of the electron given by

$$\frac{dE_e}{dt} = -\frac{4}{3}\sigma_T c\Gamma'^2 \int_{\epsilon_{\min}}^{\epsilon_{\max}} \epsilon n(\epsilon)d\epsilon \,. \tag{14}$$

We note that this formalism assumes continuous energy losses for the electrons, which is appropriate for the regime that we are considering. Furthermore, this simplified approach has the advantage that recycling cascades (in which Inverse Compton photons up-scattered to high energies are also allowed to initiate EM cascades) is more feasible than in the full Monte Carlo approach. As such, for BL Lacs, we also calculated the spectrum of second generation cascades. Notably, the effect of EM cascades is to redistribute high-energy radiation to lower energies; as such, the high-energy component of second generation cascades necessary to produce higher generation cascades is greatly reduced. Thus, the contribution from generations beyond the second generation is negligible. For FSRQs, the intrinsic spectra of the sources are sufficiently soft that even the first generation of cascades makes a small contribution to their overall collective intensity.[4] The suppression of the source brightness due to magnetic deflection of cascades (see Appendix) is also calculated, and we assume a uniform magnetic field that evolves solely due to the expansion of the Universe [$B(z) \sim B_0(1+z)^2$; Neronov & Semikoz 2009], where $B_0 \sim 5 \times 10^{-14}$ G. We should also note that for the purposes of this paper, we assume that the correlation length of the magnetic field is much larger than electron cooling distances. Alternative scenarios for the magnetic field and source spectra will be explored in future publications.

2.3 Anisotropy Energy Spectrum

The anisotropy energy spectrum, $C_\ell(E)$, is defined as the intensity fluctuation angular power (in units of sr) at a given angular scale, ℓ, as a function of energy. In the simple case of a two-component background, the total angular power is given by (Siegal-Gaskins & Pavlidou 2009)

$$C_\ell^{\mathrm{tot}} = f_1^2 C_\ell^{(1)} + f_2^2 C_\ell^{(2)} + 2f_1 f_2 C_\ell^{(1 \times 2)} \,, \tag{15}$$

where $C_\ell^{(n)}$ is the angular power spectrum of component (n), $f_n = I_n(E)/I_{\mathrm{tot}}(E)$ is the energy-dependent fraction of the total emission arising from component (n), and $C_\ell^{(n \times m)}$ is the cross-correlation term for components (n) and (m). As $C_\ell^{(n)}$ is a measure of angular fluctuations in units of the mean, it is independent of energy for a single population of sources with identical spectra. If the two components are uncorrelated, $C_\ell^{(n \times m)} = 0$, and Equation (15) is further simplified,

$$C_\ell^{\mathrm{tot}} = f_1^2 C_\ell^{(1)} + f_2^2 C_\ell^{(2)} \,. \tag{16}$$

If additional components *of negligible angular power* contribute to the total background signal, then these will not result in additional terms in Equation (16), but rather they

will affect $C_\ell^{\mathrm{tot}}(E)$ by changing the fractional contributions, f, of each of the components that *do* contribute to the angular power.

In the simple scenarios we explore, we always consider two components that do contribute to the total angular power: BL Lacs and FSRQs. Because in our adopted model the two contributions do not add up to the total EGB signal measured by *Fermi* (Abdo et al. 2010c), we assume that the rest of the EGB signal originates from a very-low C_ℓ population, such as star-forming galaxies. For simplicity, we take $C_\ell^{(\mathrm{SF})} = 0$ for this latter component. As discussed in the previous sections, the energy spectrum of the primary emission from FSRQs is very soft at very high energies, so the cascade signal from FSRQs is negligible; all cascade emission that we consider comes from reprocessed BL Lac VHE photons.

In the limit of low B, there is little angular spread in the cascade photons, so these photons appear to originate from the same sources as the primary emission. In this case, the only effect of the cascades is to alter the energy spectrum of BL Lacs, leaving their anisotropy properties unchanged. For this reason, in this scenario, we add the cascade radiation from BL Lacs to their primary emission in f_2 of Equation (16) while considering only primary emission from FSRQs in f_1; hence, the fractional components of Equation (16) become $f_1(E) = I_{\mathrm{FSRQ}}(E)/I_{\mathrm{tot}}(E)$ and $f_2(E) = [I_{\mathrm{BL\,Lac}}(E) + I_{\mathrm{casc}}(E)]/I_{\mathrm{tot}}(E)$, while the $C_\ell^{(\mathrm{FSRQ})}$ and $C_\ell^{(\mathrm{BL\,Lac})}$ remain unchanged.

In the limit of strong B ($B_0 \sim$ few $\times 10^{-14}$ G), we determined the scattering angles of the cascades (see Appendix) and found that for observed photon energies less than ~ 100 GeV, the scattering angles were sufficiently large such that within the observed angular extent of the cascade emission, the number of sources above the *Fermi*-LAT sensitivity is sufficiently large to introduce source confusion[5]. Thus, we take the cascade signal as having angular power, $C_\ell^{(\mathrm{casc})} = 0$. As such, in this scenario, we simply add the cascade emission to I_{tot}, while the numerators of f_1 and f_2 in Equation (16) still correspond to the primary (appropriately attenuated) emission from FSRQs and BL Lacs, respectively.

We have considered a range of angular scales between $\ell = 50$ and $\ell = 250$ ($\ell = 150$ with $\Delta\ell = 100$). For simplicity, we have taken $C_\ell^{(\mathrm{FSRQ})} = C_\ell^{(\mathrm{BL\,Lac})} = 6 \times 10^{-5}$ sr, which in both scenarios, gives $C_\ell^{\mathrm{tot}} \sim 10^{-5}$ sr around 1 GeV, consistent with the *Fermi* measurement of angular anisotropies in the EGB at these energies (Cuoco et al. 2011). We have calculated error bars using (Knox 1995)

$$\Delta C_\ell = \sqrt{\frac{2}{(2\ell+1)\Delta\ell f_{\mathrm{sky}}}} \left(C_\ell + \frac{C_N}{W_\ell^2} \right) \,, \tag{17}$$

where $C_N = (4\pi f_{\mathrm{sky}}/N_\gamma)$ is the photon noise angular power, and $W_\ell = \exp(-\ell^2\sigma_b^2/2)$ is the window function of a Gaussian beam. We have taken $f_{\mathrm{sky}} = 0.32$ (the unmasked fraction of the sky that would presumably be used for the anisotropy data analysis), $\sigma_b = \sigma_{68\%}/1.51$ (where $\sigma_{68\%}$ is the 68% containment angle of the *Fermi*-LAT reconstruction), and we calculate $N_\gamma = \int_{E_{\min}}^{E_{\max}} dE \frac{dI}{dE} A_{\mathrm{eff}}(E) \Omega\, t_{\mathrm{obs}}$ from the

---

[4] We note that the small amount of cascade radiation is not simply the result of the low break energy chosen for this analysis; Venters (2010) modeled FSRQ spectra as unbroken power laws up to ~ 100 TeV and also found that the FSRQ cascade contribution was small.

[5] Since the blazar contribution to the EGB is the collective emission of *unresolved* blazars, this criterion is quite conservative.
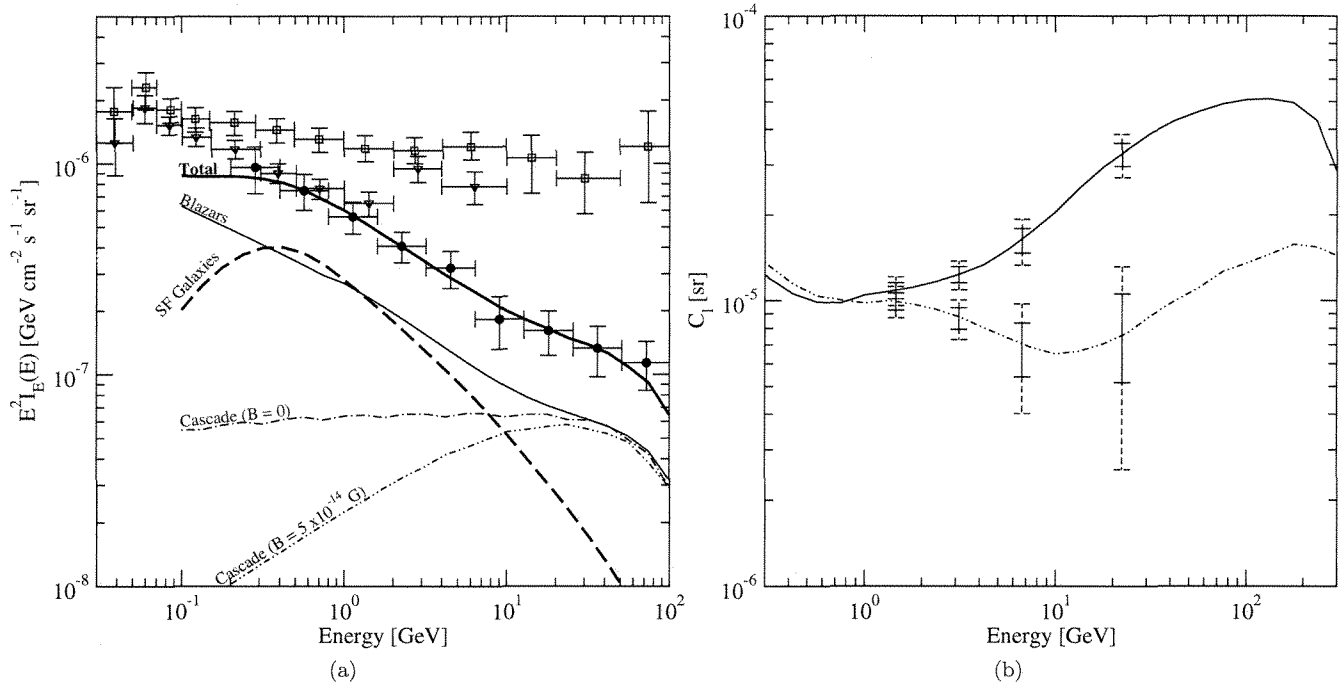
Figure 1. *a*: The spectrum of the modeled EGB (thick solid line) together with individual components: intrinsic blazar emission, including both FSRQs and BL Lacs (thin solid line); SF galaxies (dashed line); electromagnetic cascades for zero IGMF (dot-dashed line) and nonzero IGMF (double dot-dashed). For reference, the spectra of the EGB based on both *Fermi* (filled circles; Abdo et al. 2010c) and EGRET (open squares; Sreekumar et al. 1998; open triangles; Strong et al. 2004) are also plotted. *b*: The anisotropy energy spectrum of the modeled contributions to the EGB. The solid line is the total model assuming zero IGMF. The double dot-dashed line is the total model assuming nonzero IGMF. For reference, uncertainties calculated assuming five (dashed error bars) and ten (solid error bars) years of observation time are also plotted for four energy bins.

Fermi-measured EGB intensity (Abdo et al. 2010c), taking the *Fermi* effective area, $A_{\mathrm{eff}}(E)$, and $\sigma_{68\%}$ from the LAT performance curves[6] and assuming an observation time, t_{obs}, for *Fermi* of five and ten years.

3 RESULTS

In Figure 1(a), we plot the spectra of the modeled contributions to the EGB. The "total" contribution is the sum of the contributions from blazars, SF galaxies, and one of the cascade models (the total is similar for both models). The blazar component hardens above $\sim$ few GeV due to the increased contribution of BL Lacs with respect to FS-RQs, as BL Lac spectra remain hard while FSRQs soften. The cascade spectrum in the case of the zero IGMF is quite flat ($dN/dE \propto E^{-2}$) demonstrating the cascade effect of redistributing radiation from high energies to lower energies. The sum of the three components fits quite well the spectrum of the EGB as measured by *Fermi*. Notably, the spectra of the cascades for the two cases of the IGMF while similar at the highest energies are quite dissimilar at the lower energies. This is due to the loss of some cascade radiation in the strong IGMF case as significant amounts of the cascades are deflected away from the line-of-sight of the

observer. However, it should be noted that given our simple model of the blazar contribution to the the EGB, we were only able to account for cascade losses due to deflection. That is, in our simple picture, we are calculating the amount of radiation that an observer looking head-on at a given source would be able to detect. It is likely that just as cascades from one source are deflected out of the observer's line-of-sight, cascades from other sources that would otherwise be undetectable (e.g., misaligned jets) are deflected *into* the observer's line of sight. As such, the cascade intensity plotted for the strong IGMF case should be viewed as a lower limit. Nevertheless, we note that even if the strong IGMF cascade radiation were comparable to that of the zero IGMF case, the anisotropy would still be different since the angular properties of the sources would be different.

In Figure 1(b), we plot the anisotropy energy spectra of the EGB for the two cases of the IGMF. Notably, there is an appreciable difference between the two cases starting at $\sim$ few GeV. This is due to the fact that at these energies, the contribution from EM cascades relative to the other components is much more significant than at lower energies. As a result, the isotropization of the EGB due to cascades in the case of the strong IGMF is much more significant. Aiding in the distinction is that the cascades *augment* the anisotropy in the case of zero IGMF, because they enhance the contribution of the most-anisotropic component. Also plotted are uncertainties for four bins in energy calculated assuming five and ten years of observation time. The uncertainties indicate

[6] http://www.slac.stanford.edu/exp/glast/groups/canda/lat_Performance.htm

that perhaps within five, and certainly within ten, years of observations, *Fermi* will be able to distinguish between at least these two extreme cases.

4   DISCUSSION & CONCLUSION

We have studied the effect of a strong IGMF on EM cascades from blazars and the resulting impact on the cascade component of the EGB and the anisotropy energy spectrum of the EGB. We have shown that while the spectrum of cascade radiation in the case of zero IGMF is flat in E^2, the spectrum in the case of a strong IGMF is suppressed at low energies, though there could be some additional contribution arising from radiation deflected into the line-of-sight of the observer. Interestingly, in such a case, radiation that was initially emitted away from the observer and would not be observable in the case of zero IGMF could, in principle, be observable in the nonzero IGMF scenario. As such, a definitive indication of a nonzero IGMF could have profound implications for the components of the EGB. We will address this possibility in a future publication.

For the two extreme cases of IGMF strength we have considered here, we have calculated the anisotropy energy spectrum of the EGB. In the case of zero IGMF, the effect of cascades is to *augment* the anisotropy arising from blazars since the cascades increase the contribution to the EGB arising from blazars as they are highly collimated with the primary emission. In the case of the strong IGMF, the cascades are deflected substantially and the angular properties of the parent blazar population are blurred. Thus, in the case of a strong IGMF, the effect of cascades is to *reduce* the anisotropy of the EGB as they hinder the anisotropy arising from blazars rather than reinforcing it. At energies at which the relative contribution to the EGB arising from EM cascades is significant, the anisotropy energy spectra of the two cases become distinguishable. We have also calculated the uncertainties in the anisotropy energy spectra in four bins of energy assuming observation times of five and ten years with *Fermi*. Within a few short years, *Fermi* will be able to use this technique to distinguish between the two cases and constrain the IGMF.

We note that an advantage of our approach is that rather than focusing on a few select sources, our method employs information from the whole observable sky. As such, our approach could prove capable of providing more sensitive constraints on the *global* properties of the IGMF. Furthermore, our approach is not limited to uniform magnetic fields with large coherent lengths; other field configurations can be probed with this technique. In practice, in order to use this technique to provide an IGMF measurement, intermediate cases of IGMF strength need to be considered as well, and the uncertainties entering the calculation of the expected anisotropy energy spectra in each case carefully evaluated. In the case of intermediate IGMF strengths, a numerical simulation of the expected angular power is appropriate, as the cascade radiation will have somewhat, but not completely, suppressed angular anisotropy at small scales compared to the primary BL Lac emission, which will in addition be *correlated* with the latter. As such, for intermediate IGMF strengths, a simple analytical calculation of the cascade effect on the total angular power is not possible. Concerning

uncertainties, these enter our calculation primarily through the model assumptions for each EGB component (which can in turn self-consistently determine their anisotropy properties, a calculation which we have not performed here), and through the EBL model. We will expand our investigation of the practical usage of the anisotropy energy spectrum of the EGB to constrain the properties of the IGMF in future publications.

In the meantime, what this simple, proof-of-concept calculation has already demonstrated is that the anisotropy energy spectrum can be a powerful tool in constraining the IGMF. With a few more years of data from *Fermi*, we can begin to probe the IGMF and uncover more clues into the origins of ultra-high energy cosmic rays and large-scale structure formation.

REFERENCES

Abazajian K. N., Blanchet S., Harding J. P., 2011, Phys. Rev. D, 84, 103007
Abdo A. A., et al., 2010a, ApJL, 709, L152
Abdo A. A., et al., 2010b, ApJ, 723, 1082
Abdo A. A., et al., 2010c, Phys. Rev. Lett., 104, 101101
Abdo A. A., et al., 2010d, ApJ, 720, 435
Abdo A. A., et al., 2010e, ApJ, 715, 429
Aharonian F. A., et al., 2001, A&A, 366, 746
Aleksić J., et al., 2010, A&A, 524, A77
Ando S., 2009, Phys. Rev. D, 80, 023520
Ando S., Komatsu E., Narumoto T., Totani T., 2007, Phys. Rev. D, 75, 063519
Ando S., Kusenko A., 2010, ApJL, 722, L39
Ando S., Pavlidou V., 2009, MNRAS, 400, 2122
Blumenthal G. R., Gould R. J., 1970, Rev. of Mod. Phys., 42, 237
Coppi P., Aharonian F. A., 1997, ApJL, 487, L9
Cuoco A., Linden T., Mazziotta M. N., Siegal-Gaskins J. M., Vitale V., for the Fermi-LAT Collaboration Komatsu E., 2011, ArXiv e-prints, 1110.1047
Dermer C. D., Cavadini M., Razzaque S., Finke J. D., Chiang J., Lott B., 2011, ApJL, 733, L21
Essey W., Ando S., Kusenko A., 2011, Astropar. Phys., 35, 135
Fields B. D., Pavlidou V., Prodanović T., 2010, ApJL, 722, L199
Franceschini A., Rodighiero G., Vaccari M., 2008, A&A, 487, 837

Hensley B. S., Siegal-Gaskins J. M., Pavlidou V., 2010, ApJ, 723, 277

Hopkins P. F., Younger J. D., Hayward C. C., Narayanan D., Hernquist L., 2010, MNRAS, 402, 1693

Inoue Y., 2011, ApJ, 733, 66

Inoue Y., Totani T., 2009, ApJ, 702, 523

Kneiske T. M., Mannheim K., 2008, A&A, 479, 41

Knox L., 1995, Phys. Rev. D, 52, 4307

Longair M. S., 2008, Galaxy Formation. Springer

Makiya R., Totani T., Kobayashi M. A. R., 2011, ApJ, 728, 158

Neronov A., Semikoz D. V., 2009, Phys. Rev. D, 80, 123012

Neronov A., Semikoz D. V., Tinyakov P. G., Tkachev I. I., 2011, A&A, 526, A90

Neronov A., Vovk I., 2010, Science, 328, 73

Pavlidou V., Fields B. D., 2002, ApJL, 575, L5

Siegal-Gaskins J. M., 2008, JCAP, 10, 40

Siegal-Gaskins J. M., Pavlidou V., 2009, Physical Review Letters, 102, 241301

Siegal-Gaskins J. M., Reesman R., Pavlidou V., Profumo S., Walker T. P., 2011, MNRAS, 415, 1074

Sreekumar P., et al., 1998, ApJ, 494, 523

Stecker F. W., Salamon M. H., 1996, ApJ, 464, 600

Stecker F. W., Venters T. M., 2011, ApJ, 736, 40

Strong A. W., Moskalenko I. V., Reimer O., 2004, ApJ, 613, 956

Taoso M., Ando S., Bertone G., Profumo S., 2009, Phys. Rev. D, 79, 043521

Taylor A. M., Vovk I., Neronov A., 2011, A&A, 529, A144

Venters T. M., 2010, ApJ, 710, 1530

Venters T. M., Pavlidou V., 2011, ApJ, 737, 80

Venters T. M., Pavlidou V., Reyes L. C., 2009, ApJ, 703, 1939

APPENDIX A: SUPPRESSION OF THE SOURCE BRIGHTNESS DUE TO MAGNETIC DEFLECTION OF EM CASCADES

In calculating the suppression of the source brightness due to magnetic deflection of EM cascades, we must determine the angular spread of the cascades, $\theta_{\rm src}$, as viewed by a fundamental observer at the source redshift, $z_{\rm src}$ (Figure A1(a)). In order to determine $\theta_{\rm src}$ for multiple cascades, we begin with considering the problem for one generation of cascades (Figure A1(b)). In this case, θ_1, the angular spread of the cascade as viewed by a fundamental observer at z_1, can be expressed in terms of quantities evaluated at the redshift of interaction of the "primary" photon, z_2, and the angular diameter distance from $z_{\rm src} = z_1$ to z_2, $D_A(z_1, z_2)$:

$$\theta_1 = \frac{d_2}{D_A(z_1, z_2)}, \qquad (A1)$$

where d_2 is the proper lateral distance the electron has traveled as measured by a fundamental observer at z_2 (see e.g., Longair 2008), and we are neglecting Klein-Nishina effects, so the electron cooling distance, d_2^e, is not cosmological (i.e., $z_3 \approx z_2$). By geometry, d_2 is given by

$$d_2 = l_2^e \sin \delta_2 = 2r_2^L \sin^2 \delta_2, \qquad (A2)$$

where l_2^e is the straight path of d_2^e, r_2^L is the Larmor radius at z_2 of an electron with energy, E_2^e, in magnetic field of

strength, $B(z_2) = B_0(1+z_2)^2$, given by (Neronov & Semikoz 2009)

$$r_2^L = (3 \times 10^{28}\ {\rm cm}) \left[\frac{B(z_2)}{10^{-18}\ {\rm G}} \right]^{-1} \left(\frac{E_2^e}{10\ {\rm TeV}} \right), \qquad (A3)$$

and $\delta_2 = (1/2)\,\theta_2^e$ is angle through which the electron is deflected away from the straight-line path of the "primary" photon, which is equal to half of the magnetic deflection angle of the electron given by (Neronov & Semikoz 2009)

$$\theta_2^e = \frac{d_2^e}{r_2^L} = (3 \times 10^{-6})\,(1+z_2)^{-2} \left(\frac{B_0}{10^{-18}\ {\rm G}} \right) \left(\frac{E_2^e}{10\ {\rm TeV}} \right)^{-2}. \qquad (A4)$$

The angular diameter distance from z_1 to z_2 can be found from the angular diameter distance from z_2 to z_1 through the Reciprocity Theorem:

$$D_A(z_1, z_2) = \frac{1+z_1}{1+z_2} D_A(z_2, z_1), \qquad (A5)$$

where $D_A(z_2, z_1)$ for a flat universe is given by

$$D_A(z_2, z_1) = \frac{1}{1+z_1} \left[D_c(z_1) - D_c(z_2) \right], \qquad (A6)$$

and $D_c(z)$ is the comoving distance at z.

Now that we have θ_1 in terms of known quantities, we can find $\theta_{\rm src}$ for two generations of cascades using an equation similar to Equation A1. Returning to Figure A1(a), we note that in this case, the primary photon is emitted at $z_{\rm src}$ and interacts at z_1 emitting electron-type particles that do not propagate cosmological distances. One electron-type particle is deflected away from the straight-line path of the primary particle through an angle, δ_1, and up-scatters CMB photons. The up-scattered photons then propagate until they interact at z_2, creating more electron-type particles. Since we are neglecting generations of cascades higher than the second generation, we have θ_1 from the formalism developed above. The angle through which the electron at z_1 is deflected away from the straight-line path of the primary photon, δ_1, is also given by Equation A4, but for quantities evaluated at z_1.

Having found θ_1 and δ_1, we have the total angular spread of the cascades as viewed by a fundamental observer at z_1, $\theta_1^t = \theta_1 + \delta_1$. The lateral spread of the cascade as measured by a fundamental observer at z_2, D_2, is given by Equation A1:

$$D_2 = \theta_1^t D_A(z_1, z_2). \qquad (A7)$$

Finally, we can again use Equation A1 to find the angular spread of the cascades as viewed by a fundamental observer at the source redshift:

$$\theta_{\rm src} = \frac{D_2}{D_A(z_{\rm src}, z_2)}. \qquad (A8)$$

The flux suppression of the cascade due to magnetic deflection can be found from the flux of the cascade in the absence of magnetic fields by relating the solid angle of the deflected emission, $\Delta\Omega_d$, to that of the unaffected emission (in this case, the solid angle of the jet), $\Delta\Omega$:

$$F_{\Delta\Omega_d} = \frac{\Delta\Omega}{\Delta\Omega_d} F_{\Delta\Omega}. \qquad (A9)$$

We note that this procedure is only valid for non-isotropic sources. Conceptually, there should be no flux suppression for an isotropic source because the symmetry of the
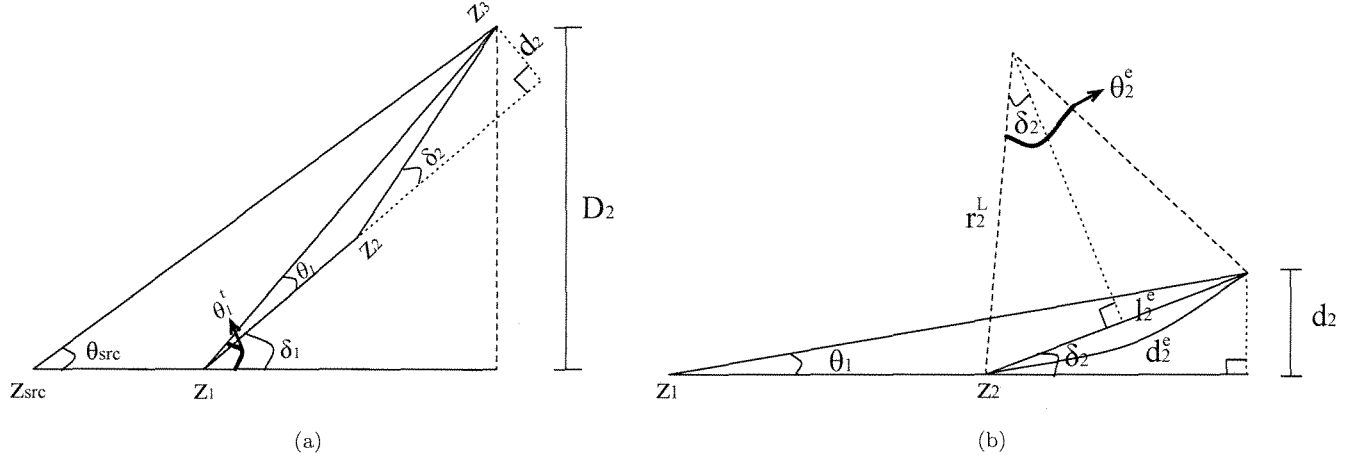
Figure 1. *a*: Geometry for the angular deflection of two generations of EM cascades. *b*: Geometry for the angular deflection of one generation of EM cascades.

problem demands that whatever emission that is deflected out of the observer's cone of sight is replaced by emission being deflected in.

This paper has been typeset from a TeX/ LaTeX file prepared by the author.